US Army Corps of Engineers®

Computing Flow through Well Screens Using an Embedded Well Technique

by Hwai-Ping Cheng

PURPOSE: The purpose of this Coastal and Hydraulics Engineering Technical Note (CHETN) is to document a computational technique developed to compute the flow rates through the screens of groundwater pumping wells or relief wells. The technique was developed for the three-dimensional (3D) groundwater (GW) flow simulation using the finite element (FE) method.

BACKGROUND: Accurate estimation of flow rates through well screens is essential in groundwater modeling and may impact decisions based on the simulation results associated with various project alternatives. In reality, the flow rate through a well screen can vary both spatially and temporally due to heterogeneity and variability present in the surrounding subsurface environment. The location of the pump within a pumping well may also impact the flow rate distribution. However, a uniform distribution of flow throughout the screen length, resulting from the total pumping rate divided by the screen length, has been often assumed and employed to characterize groundwater withdrawal in groundwater modeling due to its simplicity. This may cause inaccurate model calibration and lead to poor decisions as a result. For relief wells used to protect earthen levees, accurate estimates of flow rate through well screens under various hydrologic conditions is essential to the design of both the relief well system and the associated surface conveyance system so that excess groundwater coming out of relief wells shall be diverted efficiently, effectively, and economically.

In this CHETN, a computational technique, hereafter called the embedded well technique, developed to compute flow rates through well screens is described. This technique is applicable for groundwater flow model simulations using the finite element method. It computes for pumping wells and relief wells, at each screen-associated 3D mesh node, the mass-conservative nodal flow (Cheng et al. 2010) that represents the flow rate through the well screen section associated with the node. The technique accounts for scenarios that include or ignore the head losses across the well screen and along the well. The technique is verified with a simple box model that contains one pumping well and one relief well.

METHODOLOGY: To solve the coupled groundwater/well flow system using the finite element method, it is convenient to represent each well with multiple nodes sitting along the centerline of the well (Konikow et al. 2009), where each well node has a corresponding subsurface node sharing the same coordinates, as shown in Figure 1. In the figure, the well is represented with nine well nodes, where the top five nodes are associated with the well casing and the bottom four nodes with the well screen. Each well node is associated with a corresponding 3D GW node, where GW node IDs are presented in red color, well node IDs are presented in blue color, and the well screen is highlighted using a green shade.

Report Documentation Page

Form Approved
OMB No. 0704-0188

1. REPORT DATE	2. REPORT TYPE	3. DATES COVERED
AUG 2015		**00-00-2015 to 00-00-2015**

4. TITLE AND SUBTITLE	5a. CONTRACT NUMBER
Computing Flow through Well Screens Using an Embedded Well Technique	5b. GRANT NUMBER
	5c. PROGRAM ELEMENT NUMBER
6. AUTHOR(S)	5d. PROJECT NUMBER
	5e. TASK NUMBER
	5f. WORK UNIT NUMBER
7. PERFORMING ORGANIZATION NAME(S) AND ADDRESS(ES) **U.S. Army Engineer Research and Development Center,Vicksburg,,MS**	8. PERFORMING ORGANIZATION REPORT NUMBER
9. SPONSORING/MONITORING AGENCY NAME(S) AND ADDRESS(ES)	10. SPONSOR/MONITOR'S ACRONYM(S)
	11. SPONSOR/MONITOR'S REPORT NUMBER(S)

12. DISTRIBUTION/AVAILABILITY STATEMENT
Approved for public release; distribution unlimited

13. SUPPLEMENTARY NOTES

14. ABSTRACT

15. SUBJECT TERMS

16. SECURITY CLASSIFICATION OF:			17. LIMITATION OF ABSTRACT	18. NUMBER OF PAGES	19a. NAME OF RESPONSIBLE PERSON
a. REPORT **unclassified**	b. ABSTRACT **unclassified**	c. THIS PAGE **unclassified**	**Same as Report (SAR)**	**23**	

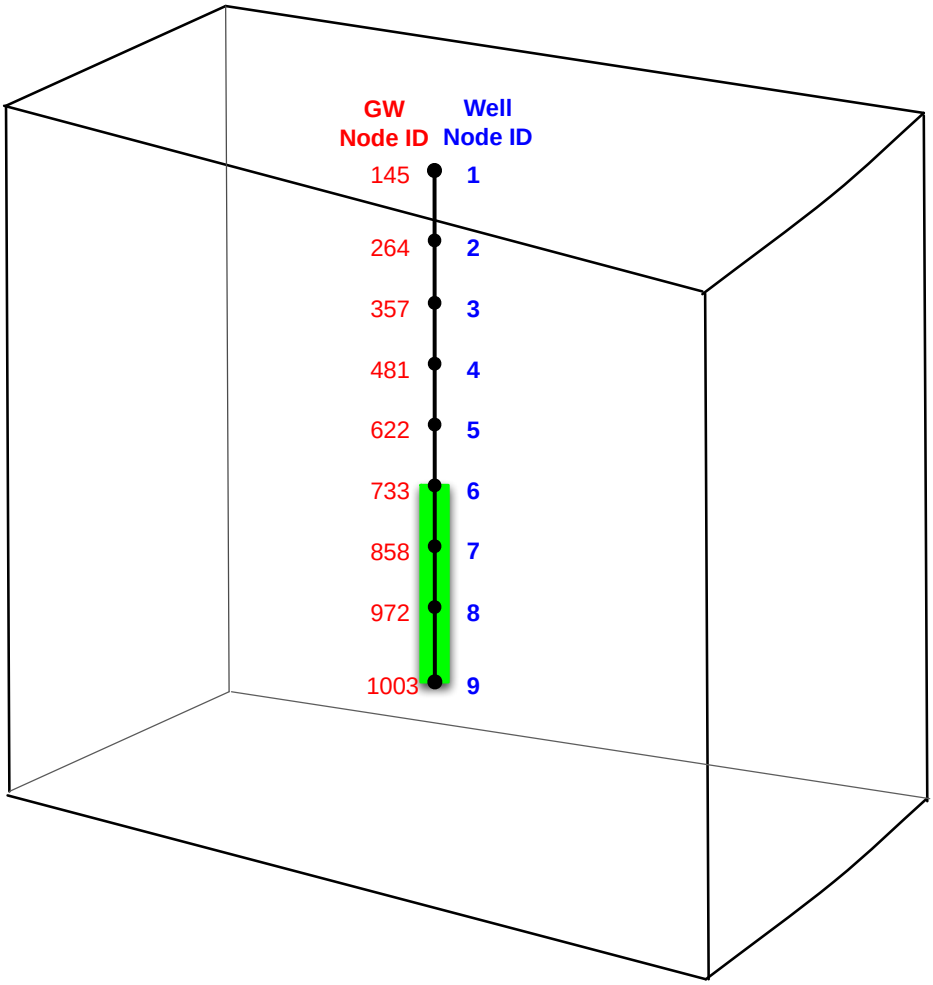

Figure 1. Example of a multinode well and its associated 3D GW nodes.

The embedded well technique computes both GW heads and well heads at model mesh nodes. It solves the governing equations of the coupled GW/well system that include the 3D Richards equation for subsurface flow and a one-dimensional (1D) steady-state equation for well flow. The Richards equation can be written as

$$\frac{\partial \theta}{\partial t} + \nabla \cdot \mathbf{V}^{GW} = Q^{GW} + R^{GW} \tag{1}$$

where θ is moisture content [L^3/L^3], t is time, ∇ is the del operator, $\mathbf{V}^{GW}$ is Darcy velocity [L/t], Q^{GW} is the source/sink [$L^3/(L^3t)$] of the GW system due to GW/well interaction, and R^{GW} represents the other sources/sinks [$L^3/(L^3t)$] of the GW system.

With the Darcy's law, $\mathbf{V}^{GW} = -\mathbf{K}^{GW} \cdot \nabla H^{GW}$, Equation 1 can be further written as

$$\frac{\partial \theta}{\partial t} - \nabla \cdot \left(\mathbf{K}^{GW} \cdot \nabla H^{GW} \right) = Q^{GW} + R^{GW} \tag{2}$$

where $\mathbf{K}^{GW}$ is GW hydraulic conductivity tensor [L/t], H^{GW} is GW total head [L].

The flow pattern within a well can be complex and nonlinear when withdrawal or injection is initiated. To resolve the temporal variation of the well flow pattern accurately, it is necessary to solve the continuity equation and the momentum equation using small time-steps. With the assumption that the well flow reaches equilibrium much quicker than the surrounding local GW flow, a 1D linear steady-state flow equation is employed to represent well flow in the coupled GW/well system so that much greater time-steps can be used for computation. The 1D steady-state well equation can be written as

$$A^{well}\frac{dV^{well}}{dl^{well}} = Q^{well} + R^{well} \tag{3}$$

where A^{well} is the cross-sectional area of the well [L^2], V^{well} is well flow velocity [L/t], l^{well} is the axis along well, Q^{well} represents the source/sink [L^3/(Lt)] of the well system due to GW/well interaction, and R^{well} represents the other source/sink [L^3/(Lt)] of the well system.

Substituting $V^{well} = -K^{well}\frac{dH^{well}}{dl^{well}}$ into Equation 3 yields

$$-A^{well}\frac{d\left(K^{well}\frac{dH^{well}}{dl^{well}}\right)}{dl^{well}} = Q^{well} + R^{well} \tag{4}$$

where K^{well} represents the equivalent hydraulic conductivity [L/t] of the well and H^{well} is well total head [L].

The subsurface flow system and the well system are coupled via the continuity of flux that simply states that water leaving the GW system is equal to water entering the well system, and vice versa, at any well locations and any times, as shown in Equation 5.

$$Q_K^{well}(t) = -Q_K^{GW}(t) \tag{5}$$

where $Q_K^{well}(t)$ is the net flow rate [L^3/t] entering the well at a well location *K* and time *t*, $Q_K^{GW}(t)$ is the net flow rate [L^3/t] entering the GW system at the same location and time.

Finite Element Discretization. Through the FE discretization, the GW equation expressed with Equation 2 can be approximated (Lin et al. 1997) as

$$\sum_K a_{I,K}^{GW} h_K^{GW} - b_I^{GW} = Q_I^{GW} + R_I^{GW} \qquad I \in N_{GW} \tag{6}$$

where N_{GW} is the total number of 3D GW nodes, *I* denotes the equation associated with GW node I, *K* denotes a GW node that belongs to an element containing node I, h_K^{GW} is the pressure

head [L] of GW node K, $a_{I,K}^{GW}$ and b_I^{GW} are coefficients resulting from matrix assembly in the finite element discretization, Q_I^{GW} represents the nodal source [L^3/t] from well, and R_I^{GW} represents the nodal source [L^3/t] via the other means, which is usually zero when GW node I is associated with the well screen.

Likewise, the well equation expressed with Equation 4 can be approximated as

$$\sum_L a_{J,L}^{well} h_L^{well} - b_J^{well} = Q_J^{well} + R_J^{well} \qquad J \in N_{well} \tag{7}$$

where N_{well} is the total number of 1D well nodes, J denotes the equation associated with well node J, L denotes a well node that belongs to a 1D element around node J, h_L^{well} is the pressure head [L] of well node L, $a_{J,L}^{well}$ and b_J^{well} are coefficients resulting from assembling the matrix in the finite element discretization, Q_J^{well} represents the nodal source [L^3/t] from subsurface, and R_J^{well} represents the nodal source [L^3/t] through the other means (e.g., withdrawal from a water pump placed in a pumping well or excess groundwater leaving a relief well from top of the well.) The following continuity equations thus exist:

$$\begin{cases} Q_I^{GW} = -Q_J^{well} = 0 & \text{if well node J is associated with the casing;} \\ Q_I^{GW} = -Q_J^{well} & \text{if well node J is associated with the screen.} \end{cases} \tag{8}$$

where GW node I is associated with well node J.

Computing Nodal Flow. When the Galerkin FE method (Miller et al. 1998) is employed to solve the Richards equation, the residual associated with each node can be computed by substituting the computed pressure head back into the global matrix equation (i.e., the left-hand side of Equation 6) that is constructed from the FE matrix assembly without taking into account boundary conditions and source/sink terms (Cheng et al. 2010). If the node is an internal node, the computed residual will be smaller than the specified residual error tolerance. If this node is a boundary node, the computed residual represents the net flow entering or leaving the GW computational domain through the boundary face area associated with the node. If this node is a point source or sink in the domain, then the computed residual is the injection or withdrawal rate via the node. Therefore, the computed residual of a screen-associated GW node represents the net flow from GW to well (when the residual is negative) or from well to GW (when the residual is positive) at the GW node. By summing up the flow rates of all GW nodes associated with the screen of a well, the total flow rate from GW to well is thus calculated, as illustrated in Figure 2 where Equation 8 is employed to determine $Q1_k^{well}$, $Q2_k^{well}$, $Q3_k^{well}$, $Q4_k^{well}$, and $Q5_k^{well}$ at each well screen node, in which k denotes the local well node ID. As shown in Figure 2, the net flow rate from GW to well will be equal to the rate of outflow at a relief well or the specified pumping rate at a pumping well, as a steady well flow is assumed.

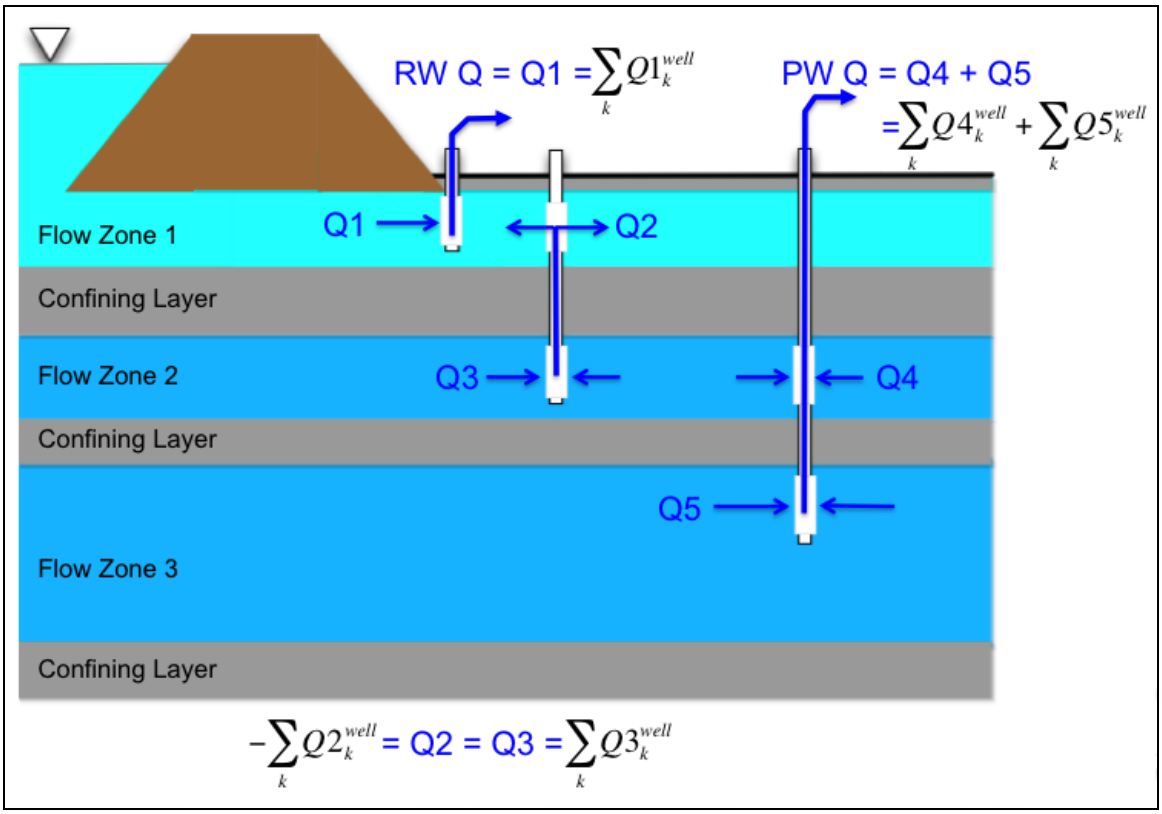

Figure 2. Concept of using mass-conservative GW nodal flow to compute flow rates through well screens and to derive the outflows of relief wells.

Head Loss across the Well Screen. When the head loss across the well screen is not negligible, the flow rate across the well screen can be computed using Equation 9:

$$Q_J^{well} = -Q_I^{GW} = A_J^{well\_screen} \cdot \frac{H_I^{GW} - H_J^{well}}{E_J^{well\_screen}} \tag{9}$$

where well node J is associated with the well screen, GW node I is associated with well node J, H_I^{GW} is the total head of GW node I, H_J^{well} is the total head of well node J, $E_J^{well\_screen}$ is the equivalent resistance across the well screen associated with well node J, $A_J^{well\_screen}$ is the equivalent screen area associated with well node J that can be further expressed as $2\pi r^{well} L_J^{well\_screen}$ with r^{well} the radius of the well and $L_J^{well\_screen}$ the equivalent length of the well screen associated with well node J, provided that the thickness of well screen packing is relatively small when compared to the radius of the well.

Applying the Darcy's law for radial, steady-state flow to a well yields Equation 10:

$$Q = -2\pi K r \cdot \frac{dH}{dr} \tag{10}$$

where H is total head, r is the distance in the radial direction, Q is the flow rate in the radial direction, and K is the hydraulic conductivity of the porous medium surrounding the well.

By assuming a radial flow through the well screen, H_I^{GW} and H_J^{well} in Equation 9 can be related by solving Equation 10 as

$$H_I^{GW} - H_J^{well} = \frac{Q_J^{well}}{2\pi K^{well_{screen}}} ln\left(\frac{r^{well} + 0.5d^{well_{screen}}}{r^{well}}\right) \tag{11}$$

where $K^{well_{screen}}$ and $d^{well_{screen}}$ are the equivalent hydraulic conductivity and the thickness, respectively, of well screen packing.

Substituting Equation 9 into Equation 11 yields

$$E_J^{well\_screen} = \frac{r^{well} \cdot \ln\left(\frac{r^{well} + 0.5d^{well\_screen}}{r^{well}}\right)}{K^{well\_screen}} \tag{12}$$

When the head loss across the well screen is negligible, the resistance is very small, and $\frac{A_J^{well\_screen}}{E_J^{well\_screen}}$ becomes very large. As a result, the algebraic equations of the coupled system may become ill-conditioned and difficult to solve. To overcome this difficulty, the total head at a well node is set to be the same as the total head at the associated GW node for computation, as shown in Equation 13:

$$H_I^{GW} = H_J^{well} \qquad \text{if well node J is associated with a screen.} \tag{13}$$

Head Loss along the Well. When the head loss along the well is not negligible, Equation 4 is solved to compute the head distribution along the well. To solve Equation 4, the well-known Hazen-Williams equation (i.e., Equation 14) that has been widely used to estimate the head loss in steady pipe flow can be used to estimate K^{well}:

$$h_L = L\left(\frac{Q_{pipe}}{C_{unit} \cdot C_{HW} \cdot A \cdot R^{0.63}}\right)^{1.852} \tag{14}$$

where h_L is the head loss in steady pipe flow, L is the length of the pipe, Q_{pipe} is the steady volumetric flow rate, A is the cross-sectional area of the pipe, R is the hydraulic radius of the pipe, C_{HW} is the Hazen-Williams roughness coefficient (*http://www. engineeringtoolbox.com/ hazen-williams-coefficients-d_798.html*) for the inside wall of the pipe, and C_{unit} is a unit-specific coefficient in the Hazen-Williams equation, where C_{unit} is 1.318 for U.S. customary units (foot and second) and 0.849 for SI units (meter and second).

Equation 14 can be rewritten as

$$V_{pipe} = \frac{Q_{pipe}}{A} = C_{unit} \cdot C_{HW} \cdot R^{0.63} \cdot \left| \nabla H \right|^{0.54} = \frac{C_{unit} \cdot C_{HW} \cdot R^{0.63}}{\left| \nabla H \right|^{0.46}} \cdot \nabla H \tag{15}$$

Therefore, K^{well} can be estimated using the following equation:

$$K^{well} = \frac{C_{unit} \cdot C_{HW} \cdot R^{0.63}}{\left| \nabla H \right|^{0.46}} \tag{16}$$

Because the Hazen-Williams equation is applicable when the flow velocity does not exceed 10 ft/s, one may use this velocity value to calculate K^{well} when there are not field data available for calibration. By assuming laminar flow, one may also use $Re < 2{,}100$ to calculate the flow velocity and then K^{well}, where Re is the Reynolds number.

Equation 4 would require small time-steps to solve when K^{well} is large. Because the head loss along the well becomes negligible when K^{well} is sufficiently large, the hydrostatic condition, as described in Equation 17, can be employed for computation so that reasonably large time-steps can be used. The entire well system in this case can be thought of as a super mixer within which the hydrostatic condition is reached immediately under any disturbances.

$$H_J^{well} = H^{well} \tag{17}$$

In addition, Equation 18 that describes mass conservation for the well is used to close the computational system:

$$Q_{outflow}^{well} = \sum_{J}^{N_{screen}} Q_J^{well} = \sum_{J}^{N_{screen}} \left[A_J^{well\_screen} \cdot \frac{H_I^{GW} - H^{well}}{E_J^{well\_screen}} \right] \tag{18}$$

where H^{well} is the hydrostatic total head of the well, and $Q_{outflow}^{well}$ represents the rate of well outflow to balance out the well inflow through the well screen.

Solving the Coupled GW/Well System. Based on the discussion above for scenarios with and without the head losses across the well screen and along the well, various scenarios are discussed as follows. To help discussion, a coupled system consisting of N_{GW} groundwater nodes and one well is used, where the well contains N_{well} well nodes, which includes N_{screen} nodes associated with the well screen and N_{casing} nodes associated with the well casing. For example, in Figure 1, N_{well} = 9, N_{screen} = 4, and N_{casing} = 5. For the coupled systems with more than one well, the same modeling techniques described below can be applied directly.

With the head loss across the screen: When the head loss across the well screen is accounted for, the GW total head and the well total head at a well location can be different. In this case, the GW system and the well system are coupled with Equation 9.

If the head loss along the well is also taken into account, there will be in total (N_{GW} + N_{well}) unknowns for the coupled system, which includes N_{GW} GW nodal heads and N_{well} well heads. The equations to solve include N_{GW} Equation 6 and N_{well} Equation 7, where the well head and the associated GW head at a screen node location are related using Equation 9. Suppose there are 1,200 GW nodes for the coupled system in Figure 1, the N_{well} well heads are treated as the extra GW unknowns in the computational system, as depicted in Figure 3a.

If the head loss along the well is negligible, the hydrostatic condition (i.e., Equation 17) applies, and there is actually only one total head to be computed for the entire well. In this case, the coupled system has in total (N_{GW} + 1) unknowns, as illustrated in Figure 3b. In addition to the N_{GW} Equation 6, Equation 18 is employed to close the computational system.

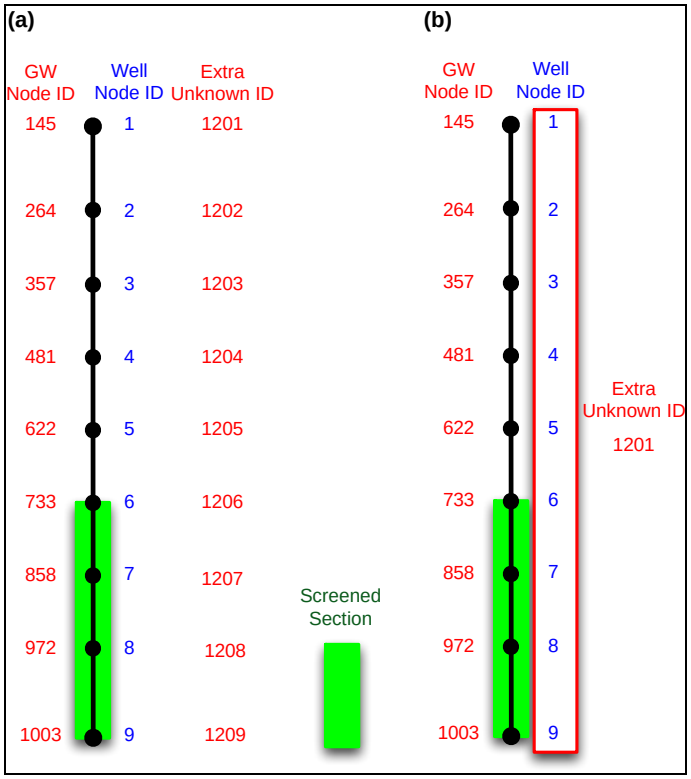

Figure 3. Numbering of unknown IDs for the coupled GW/well system when head loss across the screen is present: (a) head loss along the well also exists; (b) head loss along the well is negligible.

Without the head loss across the screen: When the head loss across the well screen is negligible, the GW total head is equal to the well total head at a screen location. In this case, the GW system and the well system are coupled with Equation 13.

If the head loss along the well is taken into account, there will be in total (N_{GW} + N_{casing}) unknowns for the coupled system because the well head and the associated GW head at each screen node location are identical. In this case, Equation 7 for well node J can be combined with Equation 6 for GW node I to form the following equation:

$$\sum_K a_{I,K}^{GW} h_K^{GW} - b_I^{GW} + \sum_L a_{J,L}^{well} h_L^{well} - b_J^{well} = R_I^{GW} + R_J^{well} \qquad I \in N_{GW}, J \in N_{screen} \tag{19}$$

where GW node I and well node J are associated with the same well location.

As a result, the number of equations will be the same as the number of unknowns. Figure 4a shows an example of the numbering system for this scenario.

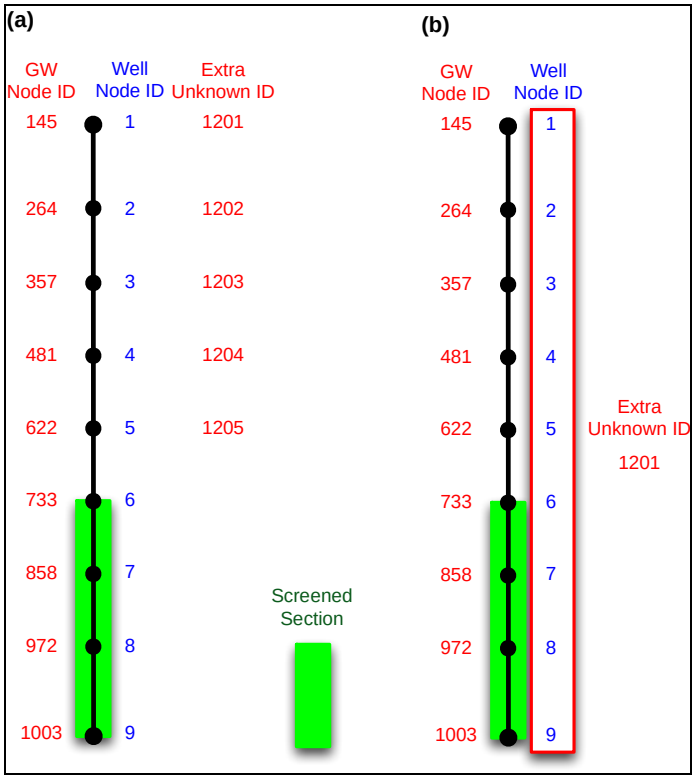

Figure 4. Numbering of unknown IDs for the coupled GW/well system when head loss across the screen is negligible: (a) head loss along the well exists; (b) head loss along the well is negligible.

If the head loss along the well is negligible, the hydrostatic condition (Equation 17) applies, and there is only one total head needed to represent the entire well as discussed previously. There are thus $(N_{screen} + 1)$ unknowns in total for the coupled system, as illustrated in Figure 4b. Because this scenario also has negligible head loss across the well screen, all GW nodes associated with the well screen are set to have a total head identical to the well total head. The entire well and all the GW nodes associated with the well screen can thus be thought of as being included in an imaginary equalizer. This further reduces the number of unknowns to $(N_{screen} + 1 - N_{screen})$. As a result, the net rate of flow entering these GW nodes is also the net rate of flow from the GW system to the well system.

To solve the coupled system, the discretized GW equations (i.e., Equation 6) of screen-associated GW nodes (e.g., 733, 858, 972, and 1003 in Figure 4b) are added up to account for the interaction between the imaginary equalizer and the surrounding GW system, which results in

$$\sum_{I \in N_{screen}^{GW}} \left(\sum_{K} a_{I,K}^{GW} h_K^{GW} - b_I^{GW} \right) = \sum_{I \in N_{screen}^{GW}} Q_I^{GW} + \sum_{I \in N_{screen}^{GW}} R_I^{GW} \tag{20}$$

where N_{screen}^{GW} represents the set of GW nodes associated with the well screen.

Equation 20 can be further written as follows using mass balance within the well at a steady state (i.e., $\sum_{J \in N_{well}} Q_J^{well} + R_J^{well} = 0$) and the continuity of flux through the GW-well interface (i.e., $\sum_{I \in N_{screen}^{GW}} Q_I^{GW} = - \sum_{J \in N_{screen}} Q_J^{well}$).

$$\sum_{I \in N_{screen}^{GW}} \left(\sum_{K} a_{I,K}^{GW} h_K^{GW} - b_I^{GW} \right) = \sum_{J \in N_{well}} R_J^{well} + \sum_{I \in N_{screen}^{GW}} R_I^{GW} \tag{21}$$

Equation 21 states the mass balance of the imaginary equalizer system. To close the computational system, Equation 13 is utilized to replace the N_{screen}^{GW} Equation 6 of well-associated GW nodes.

Boundary conditions: For solving the 3D Richards equation, both the head- and the flux-type boundary conditions can be applied. For instance, the embedded well technique has been incorporated into the 3D subsurface module of the WASH123D model (Yeh et al. 2006), WASH3D hereafter, which allows the modeler to apply Dirichlet, Cauchy, Neumann, and Variable boundary conditions to various parts of the domain boundary as necessary. As for solving the 1D steady-state well flow equation which is embedded in the 3D GW computation, a no-flow boundary condition is applied to both ends of the 1D well domain, as the pumping rate of a pumping well and the outflow rate of a relief well are treated as a source/sink term to their associated well systems (i.e., R^{well} in Equation 4).

Pump location: When a well is a pumping well, the location of the water pump in the well and the pumping schedule (i.e., the time-series of withdrawal/injection rate) are given for computation. In other words, R_J^{well} is specified, and the following equation exists:

$$\sum_{I \in N_{screen}^{GW}} Q_I^{GW} = \sum_{J \in N_{well}} R_J^{well} \tag{22}$$

As mentioned previously, Q_I^{GW} can be computed by substituting the computed heads into Equation 6, with R_I^{GW} being either zero or specified.

Relief well: Overflow at a relief well may or may not occur, depending on whether excess (i.e., high-pressure) groundwater exists around the well screen. When overflow occurs, the total head

at well top is controlled at user-specified values for computation. That is, water is assumed to flow freely from the top of the well, and the pressure head at the overflow location is assumed to be zero. When overflow ceases, the well water level is below that specified value and is computed as part of the solution. In this case, there is no flow calculated at well nodes above the well water level, and the heads at those well nodes will be undefined and excluded from computation because they are excluded from the computation.

Figure 5 depicts the flow chart of the computational algorithm for handling relief wells in the embedded well technique. As shown in the figure, for any single-step computation, which is either a steady-state computation or a transient simulation over one time-step, the user-specified total head values applied to relief wells are first examined. For relief wells where the specified total head values are greater than the given reference elevations, the specified total head values apply to the top of those relief wells as Dirichlet boundary conditions, and they are flagged as active relief wells. Otherwise, no boundary condition is applied, and the relief well is flagged as inactive even though flow is free to move in and out of the well. After the coupled GW/well system is solved for the first time, the computed head value (i.e., the initial solution in Figure 5) at the top of each relief well flagged inactive is checked. If the computed total head is greater than the given reference elevation of an inactive relief well, the relief well is flagged active. Then the given reference elevation is applied to the top of the well as a Dirichlet boundary condition in solving the coupled system for the second time. The coupled system needs to be solved the second time only when any relief wells switch from inactive to active based on the initial solution.

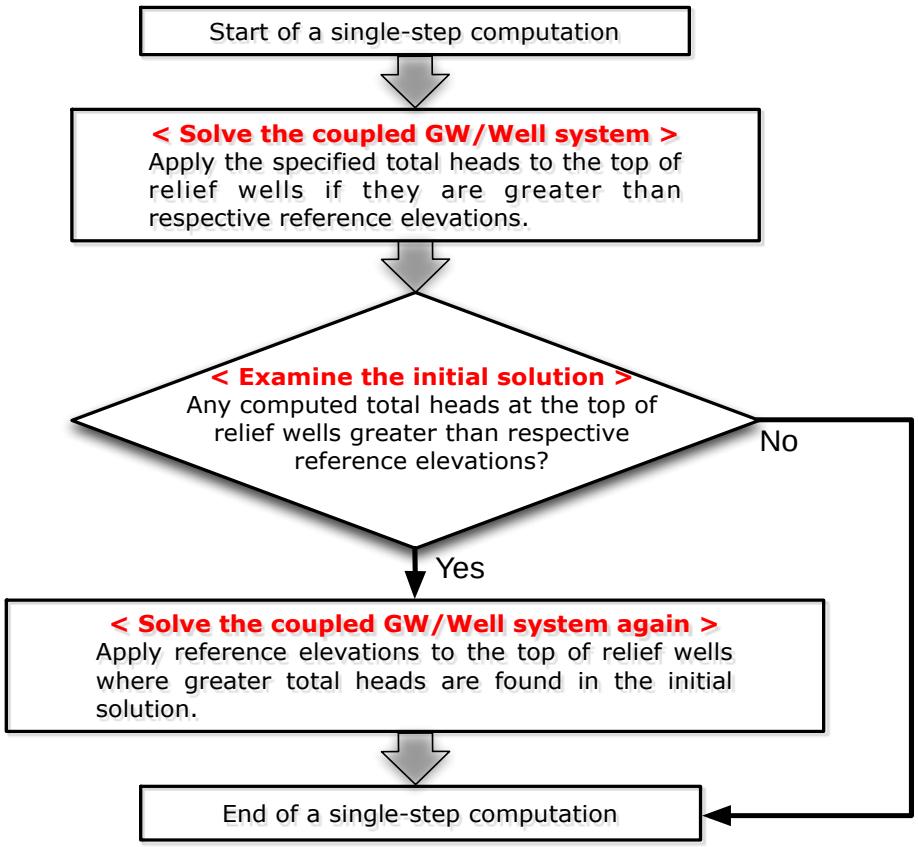

Figure 5. Flow chart to solve the coupled GW/well system when relief wells exist.

Input Data. The WASH3D model uses card input to read data needed for user-specified simulation. To account for embedded wells, RW1 and RW3 cards have been added to the input file that defines embedded relief and pumping wells, respectively, in subsurface flow simulations. An RW0 card defines a maximum saturated hydraulic conductivity value allowed for computing 1D steady flow and a minimum well screen resistance coefficient value allowed for computing head loss across the well screen. The contents of these cards are defined in Tables 1 through 3.

Table 1. Contents of RW0 card for embedded wells: 2 parameters are included.

Field	Type	Parameter Name	Parameter Description
1	Character	RW0	Card identifier for parameters for all embedded wells.
2	Positive Real	AK_RWF_MAX	Maximum saturated hydraulic conductivity value allowed for computing 1D steady flow.
3	Positive Real	R_RWF_MIN	Minimum well screen resistance coefficient value allowed for computing head loss across the well screen.

Table 2. Contents of RW1 card for embedded relief wells: 9 parameters are included.

Field	Type	Parameter Name	Parameter Description
1	Character	RW1	Card identifier for embedded relief well.
2	Positive Integer	IDRWF1(I)	ID of the embedded well corresponding to the I-th sequentially-listed embedded well that is a relief well.
3	Positive Integer	NRWNF(I)	Total number of well nodes associated with the I-th sequentially listed embedded well.
4	Positive Integer	NRWSNF(I)	Number of well screen nodes associated with the I-th sequentially listed embedded well feature that is a relief well.
5	Positive Integer	IRWTYPF(I)	ID of the x-y series to describe the time-dependent head [L] controlled at top of the well for the I-th sequentially listed embedded well.
6	Integer (0 or 1)	IDBH(I)	Index of the profile type for the I-th sequentially listed embedded well: IDBH(I) = 0, if it is a pressure head profile; IDBH(I) = 1, if it is a total head profile.
7	Positive Real	Z_RWF(I)	Reference elevation of the I-th sequentially listed embedded well, which is used to indicate whether overflow occurs at a relief well.
8	Positive Real	AK_RWF(I)	Saturated hydraulic conductivity of the I-th sequentially listed embedded well.
9	Positive Real	D_RWF(I)	Well diameter of the I-th sequentially listed embedded well.
10	Positive Real	R_RWF(I)	Well screen resistance coefficient associated with the I-th sequentially listed embedded well.

Table 3. Contents of RW3 card for embedded pumping wells: 9 parameters are included.

Field	Type	Parameter Name	Parameter Description
1	Character	RW3	Card identifier for embedded pumping well.
2	Positive Integer	IDRWF1(I)	ID of the embedded well corresponding to the I-th sequentially listed embedded well that is a relief well.
3	Positive Integer	NRWNF(I)	Total number of well nodes associated with the I-th sequentially listed embedded well.
4	Positive Integer	NRWSNF(I)	Number of well screen nodes associated with the I-th sequentially listed embedded well that is a relief well.
5	Positive Integer	IRWTYPF(I)	ID of the x-y series to describe the time-dependent pumping rate [L3/t] for the I-th sequentially listed embedded well.
6	Positive Integer	IDRWF3(I)	Location of the pump placed in the I-th sequentially listed embedded well that is a PUMPING well. For example, if IDRWF3(3,I) = 5, this pump is placed at the 5-th well node from top.
7	Positive Real	Z_RWF(I)	Reference elevation of the I-th sequentially listed embedded well, which is used to indicate whether overflow occurs at a relief well.
8	Positive Real	AK_RWF(I)	Saturated hydraulic conductivity of the I-th sequentially listed embedded well.
9	Positive Real	D_RWF(I)	Well diameter of the I-th sequentially listed embedded well.
10	Positive Real	R_RWF(I)	Well screen resistance coefficient associated with the I-th sequentially listed embedded well.

When a saturated hydraulic conductivity value (i.e., AK_RWF(I)) given in the RW1 or the RW3 card is greater than the maximum saturated conductivity allowed (i.e., AK_RWF_MAX) given in the RW0 card, head loss along the well is assumed negligible, and the hydrostatic condition is applied to the well for computation, whether it is a relief well or a pumping well. Likewise, when a well screen resistance coefficient value (i.e., R_RWF(I)) is smaller than the given minimum resistance coefficient allowed (i.e., R_RWF_MIN), head loss across the well screen is assumed negligible, and the total head at a well screen node is considered identical to that of its corresponding GW node.

To identify the groundwater nodes associated with each well and its screen section(s), two more lines are needed after each RW1 or RW3 card, and each line contains NRWNF(I) record, where NRWNF(I) is the total number of well nodes associated with the I-th sequentially listed embedded well. The first line lists the IDs of 3D GW global nodes associated with the I-th sequentially listed embedded well. These nodes are listed in order from top down along the well (i.e., the first node is the top well node, and the last node is the bottom well node). The second line defines nodes associated with the well screen and well casing of the embedded well. A screen node is indicated with an integer value of 1, while a casing node is given a value of 0. These values are also assigned to the well nodes from top down along the well.

Below is an example with both RW1 and RW3 cards for two embedded wells in a 3D GW model, where RW1 and RW3 cards define a relief well and a pumping well, respectively. As

given below, both wells are discretized using nine nodes, where the relief well has two screen sections with three nodes included in each section, and the pumping well has only one screen section that covers the bottom three nodes. Both wells account for head losses across the well screen and along the well based on the well conductivity values and the well screen resistance coefficient values given in fields 8 and 10, respectively.

```
RW0 9999.999 0.00001
RW1 1 9 6 10 1 10.0 2000.0 0.5 0.001
173 591 800 1009 1218 1427 1636 1845 2054
 0 0 1 1 1 0 1 1 1
RW3 2 9 3 12 9 10.0 5000.0 3.0 0.001
67 485 694 903 1112 1321 1530 1739 1948
 0 0 0 0 0 0 1 1 1
```

Preprocessing. A preprocessor was developed to achieve memory allocation for the specified simulation as well as to generate node connectivity information for the FE computation. Based on the data given with RW0, RW1, and RW3 cards described previously, the preprocessor determines the extra unknowns needed to account for each embedded well, which combines with the element indices information provided in the geometry file to generate node connectivity information. Table 4 lists the numbers of extra unknowns associated with various head loss scenarios for an embedded well, where the well is assumed a relief well in Figure 1. Figure 6 depicts the 3D GW nodes and extra unknowns associated with the embedded relief well for the four scenarios listed in Table 4, provided that there are 1,200 nodes in the 3D computational mesh.

Table 4. Number of extra 3D unknowns needed for an embedded relief well at various scenarios regarding head losses.

Scenario ID	RW1 Card Input	Head Loss across Screen	Head Loss along Well	Number of Extra Unknowns
1	RW1 1 9 4 10 1 10.0 2000.0 0.5 0.01 145 264 357 481 622 733 858 972 1003 0 0 0 0 0 1 1 1 1	Yes	Yes	9
2	RW1 1 9 6 10 1 10.0 20000.0 0.5 0.01 145 264 357 481 622 733 858 972 1003 0 0 0 0 0 1 1 1 1	Yes	No	1
3	RW1 1 9 6 10 1 10.0 2000.0 0.5 0.000005 145 264 357 481 622 733 858 972 1003 0 0 0 0 0 1 1 1 1	No	Yes	5
4	RW1 1 9 6 10 1 10.0 20000.0 0.5 0.000005 145 264 357 481 622 733 858 972 1003 0 0 0 0 0 1 1 1 1	No	No	1

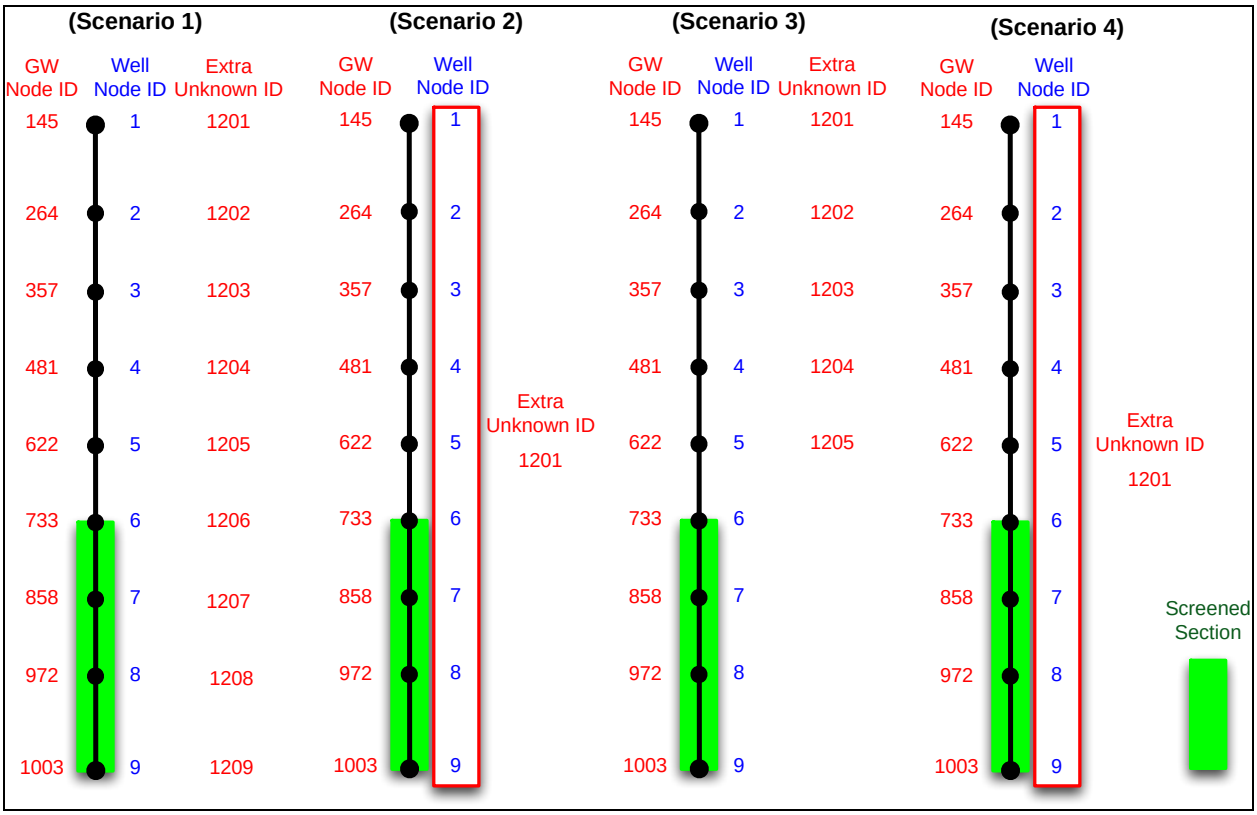

Figure 6. An example demonstrating 3D GW nodes, 1D well nodes, and extra unknowns associated with an embedded relief well at various scenarios regarding head losses.

EXAMPLE: A simple box model (Figure 7) was constructed to verify the proposed relief well algorithm.

Model Setup. As shown in Figure 7, the computational domain had a volume of $100 \times 100 \times 10$ ft^3 (x = 0 to 100 ft, y = 0 to 100 ft, and z = 0 to 10 ft) and was discretized with 2,299 nodes and 3,280 elements. The 3D mesh was composed of both hexahedral and triangular prism elements. This model had the same Dirichlet boundary conditions assigned on the right and left boundary surfaces to mimic the water levels of the nearby lake/river and variable boundary conditions on the top boundary surface to account for rainfall contribution. This box model included two embedded wells: one relief well and one pumping well (Figure 7).

A transient simulation of 10 days was conducted with the initial total head set to 10 ft for the entire domain. The rainfall rate was zero during the first 5 days and 2.54×10^{-2} ft/day during the last 5 days. The water depth on top of the relief well was set to 0 m during the first 5 days when excess groundwater came out of the well, and a water depth of 0.1 ft was controlled during the last 5 days. The variation of total heads applied to the left and right boundary faces and the pumping rate specified at the pumping well are depicted in Figure 8. The domain contained three geologic material types with saturated hydraulic conductivity values set to 30, 0.0001, and 1,000 ft/day, respectively. The modified compressibility was 0.001 for all the three material types. A simple set of soil curves for both material types was employed as shown in Figure 9. The time interval used for the transient simulation was 0.5 day throughout the simulation.

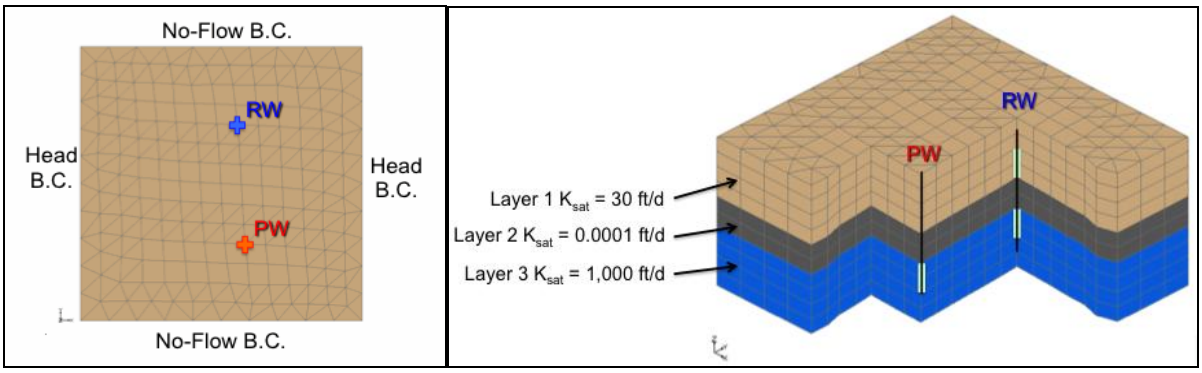

Figure 7. Plan view (left) and oblique view (right) of the box model, where z-magnification = 10.

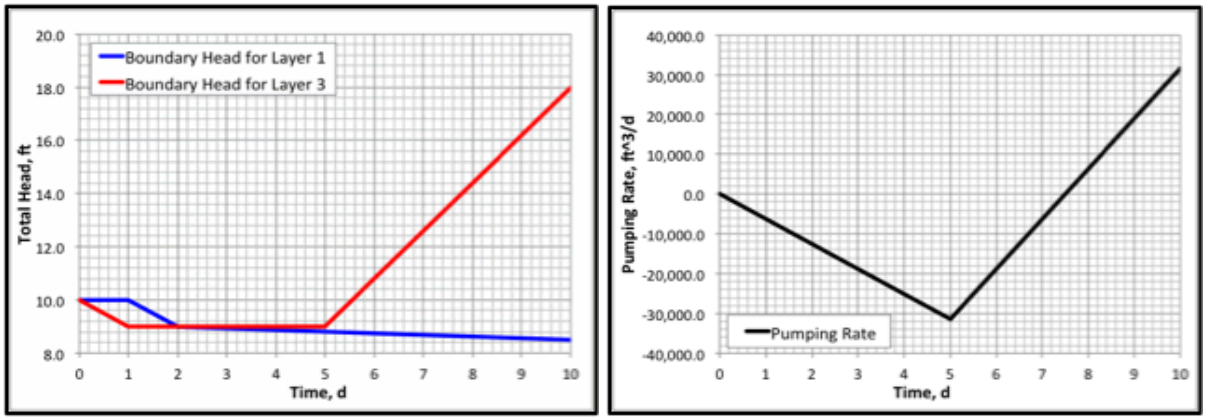

Figure 8. Head boundary conditions (left) and specified pumping rate (right) used for the box model.

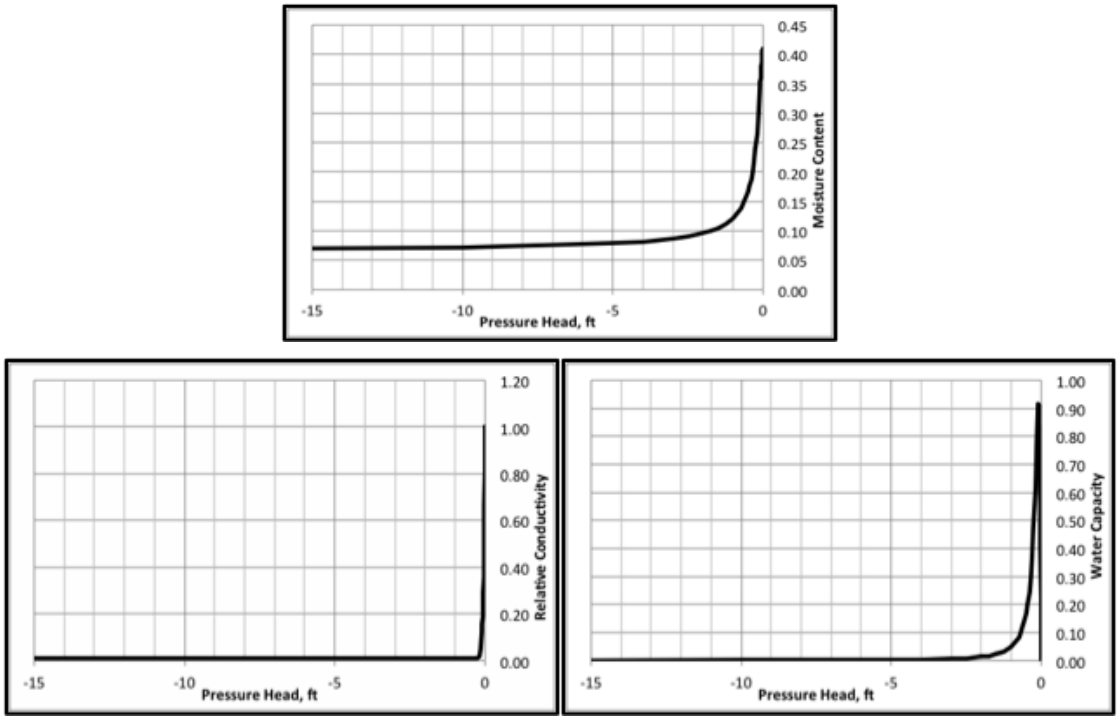

Figure 9. Soil curves used for the box model.

Results and Discussion. Four scenarios, associated with different combinations of with and without head losses along wells and across well screens, were simulated. Table 5 presents the RW1 and RW3 card input data for these scenarios, where the saturated hydraulic conductivity for well flow value (highlighted in red color) and the well screen resistance coefficient value (highlighted in blue color) were compared with the given AK_RWF_MAX (set to 9999.999) and R_RWF_MIN (set to 0.00001) values, respectively, to determine whether head loss is negligible.

Table 5. RW1 and RW3 card input data for scenarios regarding head losses.

Scenario ID	RW1/RW3 Card Input	Head Loss Across Screen	Head Loss Along Well
1	RW1 1 9 6 10 1 10.0 **2000.0** 0.5 **0.001** 173 591 800 1009 1218 1427 1636 1845 2054 0 0 1 1 1 0 1 1 1 RW3 2 9 3 12 9 10.0 **5000.0** 3.0 **0.001** 67 485 694 903 1112 1321 1530 1739 1948 0 0 0 0 0 0 1 1 1	Yes	Yes
2	RW1 1 9 6 10 1 10.0 **20000.0** 0.5 **0.001** 173 591 800 1009 1218 1427 1636 1845 2054 0 0 1 1 1 0 1 1 1 RW3 2 9 3 12 9 10.0 **50000.0** 3.0 **0.001** 67 485 694 903 1112 1321 1530 1739 1948 0 0 0 0 0 0 1 1 1	Yes	No
3	RW1 1 9 6 10 1 10.0 **2000.0** 0.5 **0.000001** 173 591 800 1009 1218 1427 1636 1845 2054 0 0 1 1 1 0 1 1 1 RW3 2 9 3 12 9 10.0 **5000.0** 3.0 **0.000001** 67 485 694 903 1112 1321 1530 1739 1948 0 0 0 0 0 0 1 1 1	No	Yes
4	RW1 1 9 6 10 1 10.0 **20000.0** 0.5 **0.000001** 173 591 800 1009 1218 1427 1636 1845 2054 0 0 1 1 1 0 1 1 1 RW3 2 9 3 12 9 10.0 **50000.0** 3.0 **0.000001** 67 485 694 903 1112 1321 1530 1739 1948 0 0 0 0 0 0 1 1 1	No	No

Tables 6 and 7 compare total head distribution at well nodes and their associated GW nodes at time = 5 days and 10 days, respectively. Figure 10 provides a visual comparison of GW total head distribution and flow directions around the two wells at both time = 5 days and 10 days. Table 8 compares the nodal flow rates, from GW to well, at well nodes at time = 5 days and 10 days, where the total well flow rate is also listed.

Table 6. Computed well and the associated GW total heads at time = 5 days.

Well Node ID	Attribute[1]	Scenario 1[2]		Scenario 2[2]		Scenario 3[2]		Scenario 4[2]	
		Well Head, ft	GW Head, ft	Well Head, ft	GW Head, ft	Well Head, ft	GW Head, ft	Well Head, ft	GW Head, ft
RW1-1	CN	N/A[3]	9.40	N/A	9.69	N/A	9.42	N/A	9.76
RW1-2	CN	9.43	9.41	9.81	9.70	9.45	9.43	9.83	9.77
RW1-3	SN	9.43	9.43	9.81	9.75	9.45	9.45	9.83	9.83
RW1-4	SN	9.46	9.46	9.81	9.78	9.48	9.48	9.83	9.83
RW1-5	SN	9.52	9.50	9.81	9.79	9.53	9.53	9.83	9.83
RW1-6	CN	9.66	9.66	9.81	9.62	9.68	9.65	9.83	9.62
RW1-7	SN	9.81	9.84	9.81	9.83	9.84	9.84	9.83	9.83
RW1-8	SN	9.84	9.84	9.81	9.83	9.84	9.84	9.83	9.83
RW1-9	SN	9.84	9.84	9.81	9.83	9.84	9.84	9.83	9.83
RW3-1	CN	15.92	9.17	16.48	9.18	14.49	9.17	14.68	9.18
RW3-2	CN	15.92	9.17	16.48	9.18	14.49	9.17	14.68	9.18
RW3-3	CN	15.92	9.17	16.48	9.18	14.49	9.17	14.68	9.18
RW3-4	CN	15.92	9.17	16.48	9.18	14.49	9.17	14.68	9.18
RW3-5	CN	15.92	9.17	16.48	9.18	14.49	9.17	14.68	9.18
RW3-6	CN	15.92	10.30	16.48	10.30	14.49	10.24	14.68	10.26
RW3-7	SN	15.92	15.02	16.48	14.99	14.49	14.49	14.68	14.68
RW3-8	SN	16.16	14.85	16.48	14.89	14.56	14.56	14.68	14.68
RW3-9	SN	16.75	14.52	16.48	14.50	14.78	14.78	14.68	14.68

[1] CN = casing node; SN = screen node.
[2] Scenario 1: head loss along the well and across the screen;
Scenario 2: head loss across the screen only;
Scenario 3: head loss along the well only;
Scenario 4: negligible head losses.
[3] N/A denotes the well water level is lower than the elevation of the well node.

As can be seen from Tables 6 and 7, the water level at a well node (i.e., well head) was the same as the total head of the associated GW node when the well node was located within a screen section with negligible head loss across the screen (i.e., Scenarios 3 and 4). The well head was different from the GW total head of the associated GW node when either the well node was in a casing section or head loss across the screen was not negligible (i.e., Scenarios 1 and 2).

At time = 10 days, the high head applied to the boundary associated with layer 3 resulted in overflow at the relief well, where a controlled water level at 10.1 ft was set to the top of the well (i.e., well head at RW1-1, Table 7). The differences of GW total head distribution between the two wells were more obvious among scenarios, when compared with those at time = 5 days (Figure 10). In Table 8, the outflow from the relief well also varied drastically among these four scenarios, where the application of hydrostatic condition in the well (i.e., negligible head loss along well, Scenarios 2 and 4) would yield much more water drawn from GW to the well, when compared with the scenarios accounting for head loss along the well (i.e., Scenarios 1 and 3).

Table 7. Computed well and the associated GW total heads at time = 10 days.

Well Node ID	Attribute[1]	Scenario 1[2]		Scenario 2[2]		Scenario 3[2]		Scenario 4[2]	
		Well Head, ft	GW Head, ft	Well Head, ft	GW Head, ft	Well Head, ft	GW Head, ft	Well Head, ft	GW Head, ft
RW1-1	CN	10.10	11.16	10.10	9.91	10.10	11.30	10.10	9.98
RW1-2	CN	10.75	11.23	10.10	9.93	10.83	11.36	10.10	10.01
RW1-3	SN	11.39	11.42	10.10	10.01	11.56	11.56	10.10	10.10
RW1-4	SN	11.93	11.87	10.10	10.05	12.08	12.08	10.10	10.10
RW1-5	SN	12.71	12.43	10.10	10.08	12.77	12.77	10.10	10.10
RW1-6	CN	14.65	10.91	10.10	10.36	14.87	10.95	10.10	10.10
RW1-7	SN	16.58	16.98	10.10	13.62	16.96	16.96	10.10	10.10
RW1-8	SN	16.93	17.00	10.10	13.87	16.99	16.99	10.10	10.10
RW1-9	SN	16.99	17.02	10.10	14.16	17.01	17.01	10.10	10.10
RW3-1	CN	11.05	9.09	10.04	8.96	12.49	9.11	11.26	8.98
RW3-2	CN	11.05	9.09	10.04	8.95	12.49	9.11	11.26	8.96
RW3-3	CN	11.05	9.09	10.04	8.95	12.49	9.11	11.26	8.96
RW3-4	CN	11.05	9.09	10.04	8.95	12.49	9.11	11.26	8.96
RW3-5	CN	11.05	9.09	10.04	8.95	12.49	9.11	11.26	8.96
RW3-6	CN	11.05	11.23	10.04	11.18	12.49	11.15	11.26	11.06
RW3-7	SN	11.05	11.95	10.04	11.53	12.49	12.49	11.26	11.26
RW3-8	SN	10.81	12.13	10.04	11.63	12.42	12.42	11.26	11.26
RW3-9	SN	10.22	12.46	10.04	12.02	12.19	12.19	11.26	11.26

[1] CN = casing node; SN = screen node.
[2] Scenario 1: head loss along the well and across the screen;
Scenario 2: head loss across the screen only;
Scenario 3: head loss along the well only;
Scenario 4: negligible head losses.

To verify the computed flow rates via the relief well were calculated correctly, a second set of WASH3D simulations was conducted, where the GW nodes associated with well screens were treated as point sources/sinks, and their respective flow rates computed previously (e.g., those listed in Table 8) were employed as the injection/withdrawal rates. Although not shown here, the computed GW total heads were the same as those computed previously (e.g., those listed in Tables 6 and 7), which indicates that the relief well flow rates were computed accurately.

SUMMARY: This technical note describes the details of an embedded well technique developed, based on the finite element method, to compute mass-conservative nodal flow rates at screen nodes of both relief and pumping wells. The technique solves the governing equations of the coupled system of GW and embedded wells to compute the nodal flow at each well node location, where no presumed nodal flow distribution over well screen is necessary. As a result, the GW model can be better calibrated and the outflow of a relief well can be accurately estimated. This numerical technique accounts for scenarios with and without well inefficiency (i.e., head losses along the well and across the screen). This technique and an algorithm to handle the computation associated with relief wells have been incorporated into the WASH3D model and can be incorporated into other FEM-based groundwater models. A box model was employed to verify the implementation of embedded technique in WASH3D.

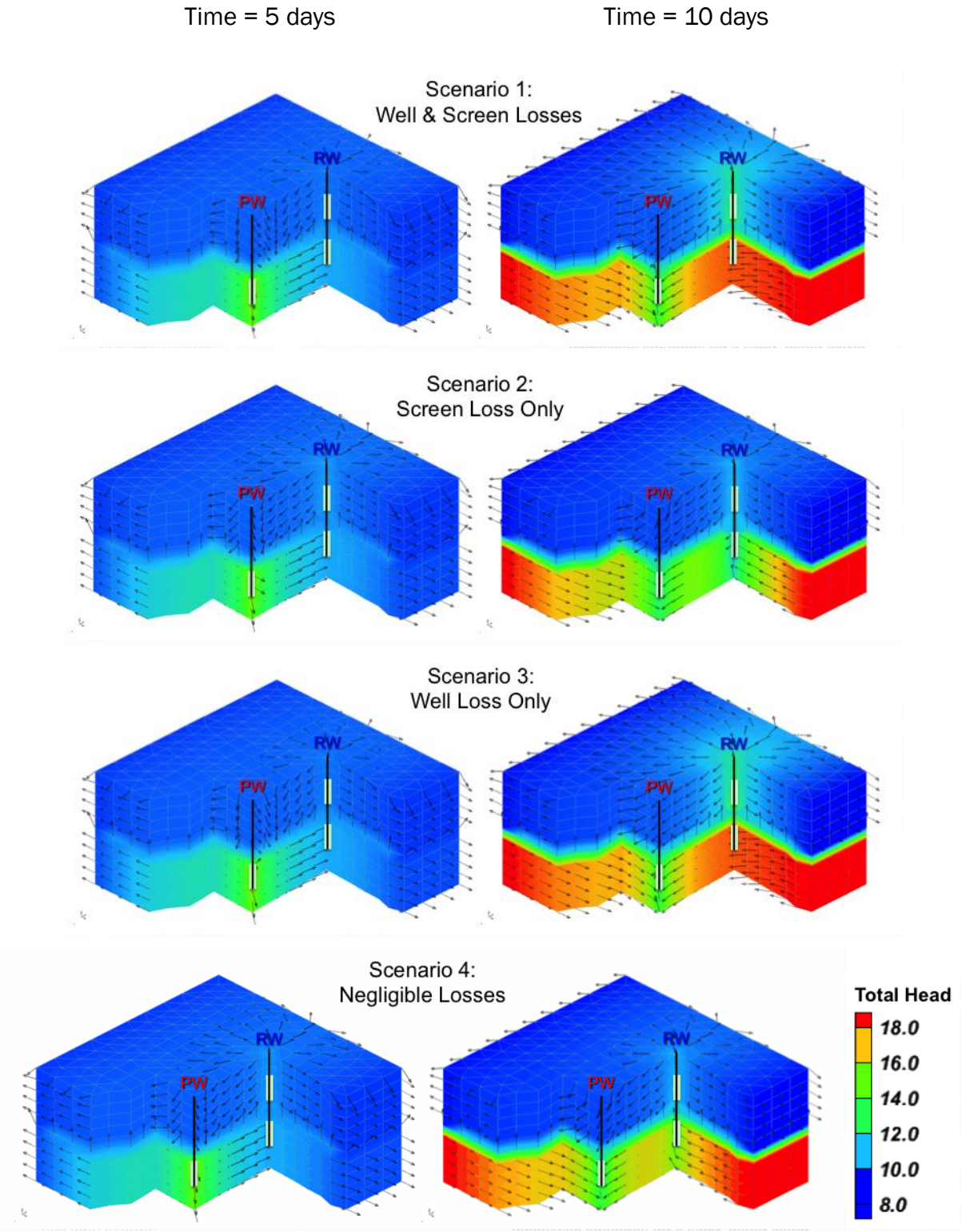

Figure 10. GW total head distribution (color code) and flow directions (arrows) around wells at time = 5 days (left images) and time = 10 days (right images), where z-magnification = 5.

Table 8. Computed flow rates of wells at time = 5 days and time = 10 days.

Well Node ID	Scenario 1[1]		Scenario 2[1]		Scenario 3[1]		Scenario 4[1]	
	Nodal Flow[2], ft³/d		Nodal Flow, ft³/d		Nodal Flow, ft³/d		Nodal Flow, ft³/d	
	5 days	10 days	5 days	10 days	5 days	10 days	5 days	10 days
RW1-1	0.00	0.00	0.00	0.00	0.00	0.00	0.00	0.00
RW1-2	0.00	0.00	0.00	0.00	0.00	0.00	0.00	0.00
RW1-3	-10.82	43.60	-44.08	-72.73	-11.47	82.60	-71.61	-115.64
RW1-4	-11.04	-97.26	-44.03	-71.95	-7.82	-69.60	-38.58	-59.18
RW1-5	-35.73	-451.66	-28.81	-46.89	-42.39	-548.70	-19.26	-29.56
RW1-6	0.00	0.00	0.00	0.00	0.00	0.00	0.00	0.00
RW1-7	47.24	622.98	55.71	8295.55	60.77	809.81	17.95	5406.38
RW1-8	8.59	113.21	39.82	5928.93	0.37	4.95	36.02	10837.20
RW1-9	1.76	23.19	21.39	3185.09	0.54	7.18	75.48	22805.20
Total Well Flow[3] (ft³/d)	0.00	254.06	0.00	17218.00	0.00	286.24	0.00	38844.30
Well Node ID	Nodal Flow, ft³/d		Nodal Flow, ft³/d		Nodal Flow, ft³/d		Nodal Flow, ft³/d	
	5 days	10 days	5 days	10 days	5 days	10 days	5 days	10 days
RW3-1	0.00	0.00	0.00	0.00	0.00	0.00	0.00	0.00
RW3-2	0.00	0.00	0.00	0.00	0.00	0.00	0.00	0.00
RW3-3	0.00	0.00	0.00	0.00	0.00	0.00	0.00	0.00
RW3-4	0.00	0.00	0.00	0.00	0.00	0.00	0.00	0.00
RW3-5	0.00	0.00	0.00	0.00	0.00	0.00	0.00	0.00
RW3-6	0.00	0.00	0.00	0.00	0.00	0.00	0.00	0.00
RW3-7	-8478.32	8478.32	-7032.01	7032.01	-2558.57	2558.57	-4361.57	4361.57
RW3-8	-12400.00	12400.00	-15043.20	15043.20	-5339.13	5339.13	-8743.83	8743.83
RW3-9	-10537.58	10537.58	-9340.69	9340.69	-23518.20	23518.20	-18310.40	18310.50
Total Well Flow[3] (ft³/d)	-31415.90	31415.90	-31415.90	31415.90	-31415.90	31415.90	-31415.90	31415.90

[1] Scenario 1: head loss along the well and across the screen;
Scenario 2: head loss across the screen only;
Scenario 3: head loss along the well only;
Scenario 4: negligible head losses.

[2] A positive nodal flow rate denotes water entering well from GW at the well node, and a negative value indicates water is from well to GW at the well node.

[3] For a relief well, a positive total well flow represents the rate of outflow at the well top; for a pumping well, a positive total flow represents its withdrawal rate, and a negative total flow represents its injection rate.

ADDITIONAL INFORMATION: This work was sponsored by the Flood & Coastal Storm Damage Reduction Program. Dr. Stacy E. Howington and Dr. Matthew W. Farthing of the U.S. Army Engineer Research and Development Center (ERDC), Coastal and Hydraulics Laboratory (CHL) provided valuable inputs. For additional information, contact Hwai-Ping (Pearce) Cheng, ERDC-CHL, 3909 Halls Ferry Road, Vicksburg, MS 39180, at 601-634-3699 or e-mail: *Hwai-Ping.Cheng@usace. army.mil*. This CHETN should be cited as follows:

Cheng, H.-P. 2015. *Computing flow through well screens using an embedded well technique*. ERDC/CHL CHETN-XI-4. Vicksburg, MS: U.S. Army Engineer Research and Development Center.

An electronic copy of this CHETN is available from *http://chl.erdc.usace.army.mil/chetn*.

REFERENCES

Cheng, J-R. C., H-P. Cheng, M. W. Farthing, and C. E. Kees. 2010. *Computing locally-mass-conservative fluxes from multi-dimensional finite element flow simulations*. ERDC TN-SWWRP-10-4. Vicksburg, MS: U.S. Army Engineer Research and Development Center. *http://acwc.sdp.sirsi.net/client/search/ asset/1004863*

Konikow, L. F., G. Z. Hornberger, K. J. Halford, and R. T. Hanson, 2009. *Revised multi-node well (MNW2) package for MODFLOW ground-water flow model: Techniques and methods 6–A30*. Reston, Virginia: U.S. Geological Survey. *http://pubs.usgs.gov/tm/tm6a30/pdf/TM-6A30_lowrez.pdf*

Lin H-C., D. R. Richards, G-T. Yeh, J-R. C. Cheng, H-P. Cheng, and N. L. Jones. 1997. *FEMWATER: A three-dimensional finite element computer model for simulating density-dependent flow and transport in variably saturated media*. CHL-97-12 Technical Report. Vicksburg, MS: U.S. Army Engineer Waterways Experiment Station.

Miller, C. T., G. Christakos, P. T. Imhoff, J. F. McBride, J. A. Pedit, and J. A. Trangenstein. 1998. Multiphase flow and transport modeling in heterogeneous porous media: Challenges and approaches. *Advances in Water Resources* 21(2):77–120.

Yeh, G.-T., G. Huang, H.-P. Cheng, F. Zhang, H.-C. Lin, E. Edris, and D. Richards. 2006. A first-principle, physics-based watershed model: WASH123D. In *Watershed Models*, ed. V. P. Singh and D. K. Frevert, 211–244. Boca Raton, FL: CRC Press, Taylor and Francis Group.